

Small-angle cross sections for $^{50,52}\text{Cr}(^3\text{He},d)^{51,53}\text{Mn}$ at 18 MeV

J. E. Park, W. W. Daehnick, and M. J. Spisak

Nuclear Physics Laboratory, University of Pittsburgh, Pittsburgh, Pennsylvania 15260

(Received 27 February 1978)

The reactions $^{50,52}\text{Cr}(^3\text{He},d)$ were investigated at an incident energy of 18 MeV with 12–15 keV resolution. Special emphasis was placed on small-angle measurements of the angular distributions, including $\theta = 0^\circ$ in order to study new $^{51,53}\text{Mn}$ levels and to document deviations from standard distorted-wave Born-approximation predictions, which appear to depend on the total-angular momentum transfer j . Absolute differential cross sections were obtained in small angular steps for $0^\circ \leq \theta \leq 45^\circ$ in ^{51}Mn and $0^\circ \leq \theta \leq 30^\circ$ in ^{53}Mn using a high-resolution position-sensitive (helix) gas counter and photographic emulsions as detectors. l -transfer assignments and spectroscopic factors were deduced from comparison with distorted-wave Born-approximation calculations for the levels up to 4.52 MeV in ^{51}Mn and up to 6 MeV excitation in ^{53}Mn . A number of new $l = 0, 1$ values were assigned in both Mn isotopes on the basis of better small-angle data. For $l = 1$, systematic differences between known $p_{1/2}$ and $p_{3/2}$ transitions were noted at angles below 10° . Distorted-wave Born approximation calculations with familiar spin orbit potentials fail to reproduce these differences.

NUCLEAR REACTIONS $^{50,52}\text{Cr}(^3\text{He},d)^{51,53}\text{Mn}$, $E_{^3\text{He}} = 18$ MeV; measured $\sigma(E_d, \theta)$, resolution ~ 13 keV. DWBA analysis, deduced l , π , spectroscopic factors, small angle $l = 1$ j dependence.

I. INTRODUCTION

In the $f_{7/2}$ shell l assignments have been reported for most low-lying levels, but relatively few j values are reliably known. It is now believed that a comparison of the experimental cross sections for (^7Li , ^6He) at small ($<5^\circ$) angles with distorted-wave Born-approximation (DWBA) predictions will determine j values, provided that the level is a singlet and its l value known.^{1,2} Empirically, angular distributions for (^7Li , ^6He) past the stripping peaks are not very characteristic of any structure effects, but at or near 0° easily recognized j dependent differences are seen. In this study the reactions $^{50,52}\text{Cr}(^3\text{He},d)$ have been measured with improved resolution for comparison with a set of correlated (^7Li , ^6He) proton transfer experiments. Tentative experimental evidence is presented that as in (d,p),³ (p,d),⁴ and (d,t) (Refs. 5, 6) reactions, experimental ($^3\text{He},d$) angular distributions not only depend on the orbital angular momentum l but also on the total angular-momentum transfer j . More generally, it is of interest to investigate how ($^3\text{He},d$) cross sections differ from DWBA calculations at small angles.⁷

Earlier studies of the stripping reaction $^{50}\text{Cr}(^3\text{He},d)$ were carried out at energies below 12 MeV (Refs. 8, 9) and for $^{52}\text{Cr}(^3\text{He},d)$ at various incident energies^{2,9-12} with energy resolution ≥ 20 keV. We have reinvestigated these reactions at 18 MeV to very small angles with ~ 13 keV energy resolution in order to obtain more reliable

l values and spectroscopic factors and simultaneously look for any small-angle j dependence of the ($^3\text{He},d$) angular distributions.

II. EXPERIMENTAL PROCEDURE

The experiments were performed with an 18 MeV $^3\text{He}^{++}$ beam from the University of Pittsburgh Van de Graaff accelerator. The targets consisted of 25 $\mu\text{g}/\text{cm}^2$ metallic ^{50}Cr (96.8% enriched) and 20 $\mu\text{g}/\text{cm}^2$ metallic ^{52}Cr (99.87% enriched) on 6 $\mu\text{g}/\text{cm}^2$ and a 10 $\mu\text{g}/\text{cm}^2$ carbon backings, respectively. ^{50}Cr targets contain 3% ^{52}Cr ; and small amounts of O, Si, Cl, and Cu contaminants are present in both chromium targets. Target thickness was measured by comparing small-angle elastic scattering off the targets used with optical-model predictions. Monitoring of beam and normalization of the data were accomplished by charge collection and simultaneous measurements of elastically scattered ^3He by Si detectors fixed at $\pm 25^\circ$ to the incident beam.

The reaction deuterons were detected and identified by a helical cathode gas proportional counter,¹³ and for large angles also with nuclear emulsions (Kodak NTB 50 μm), placed at the focal plane of an Enge split-pole spectrograph. Angular distributions were taken from 0° to 45° for ^{51}Mn and 0° to 30° for ^{53}Mn in small angular steps, especially at forward angles. Our three-section "helix" counter was most essential for

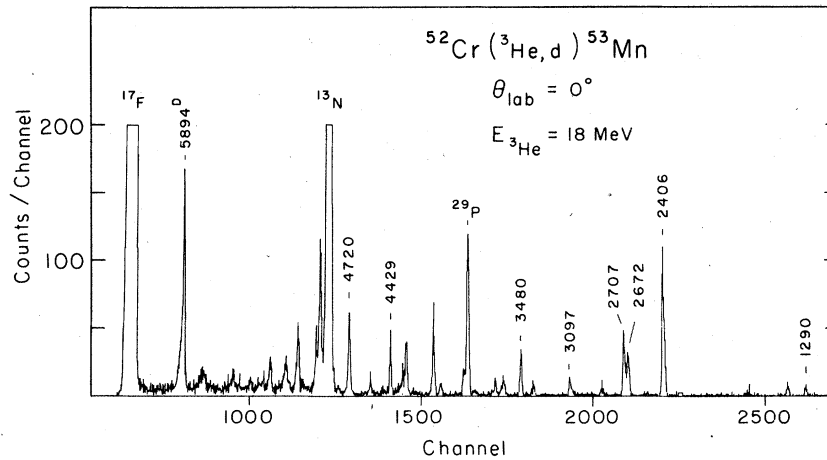


FIG. 1. Zero degree $^{52}\text{Cr}(^3\text{He},d)^{53}\text{Mn}$ spectrum obtained with helix counter. Low background counts were obtained by requiring a triple coincidence between the position, ΔE and E detectors, and computer-aided particle identification.

small-angle measurements, particularly at $\theta = 0^\circ$. A triple coincidence between the three counters: position (front) and ΔE proportional counters and an E scintillation counter and use of the E -scintillation signal for particle identification enabled us to separate different particle groups reliably, thus providing low background, high resolution spectra even at $\theta = 0^\circ$, i.e., in the direction of the direct beam. A typical 0° spectrum for $^{52}\text{Cr}(^3\text{He},d)$ taken with the helix counter is shown in Fig. 1. Figure 2 shows the plate spectrum for $^{50}\text{Cr}(^3\text{He},d)$ taken at $\theta_{\text{lab}} = 15^\circ$.

Energy resolution was 12–15 keV, and the energy calibration for the spectra was made by a direct comparison with an $^{54}\text{Fe}(^3\text{He},d)$ spectrum and with

well-known states of $^{51,53}\text{Mn}$. The same spectrograph B fields were used for both $^{50,52}\text{Cr}$ targets at a given angle in order to identify the ^{53}Mn levels appearing in ^{51}Mn spectra and to eliminate their contributions to ^{51}Mn states where the peaks from the isotopes overlap energetically. We did not take angular distributions for the well-known g.s. and 0.378 MeV state in ^{53}Mn because of the more positive Q_0 value in $^{52}\text{Cr}(^3\text{He},d)^{53}\text{Mn}$ reaction. The measured excitation energies listed in the figures and tables are believed to be accurate to ± 2 keV below 3 MeV, and to ± 3 keV above 3 MeV in ^{53}Mn and for 3–4.52 MeV in ^{51}Mn .

The cross-section uncertainties shown in Figs. 3 and 4 are due to statistics, background sub-

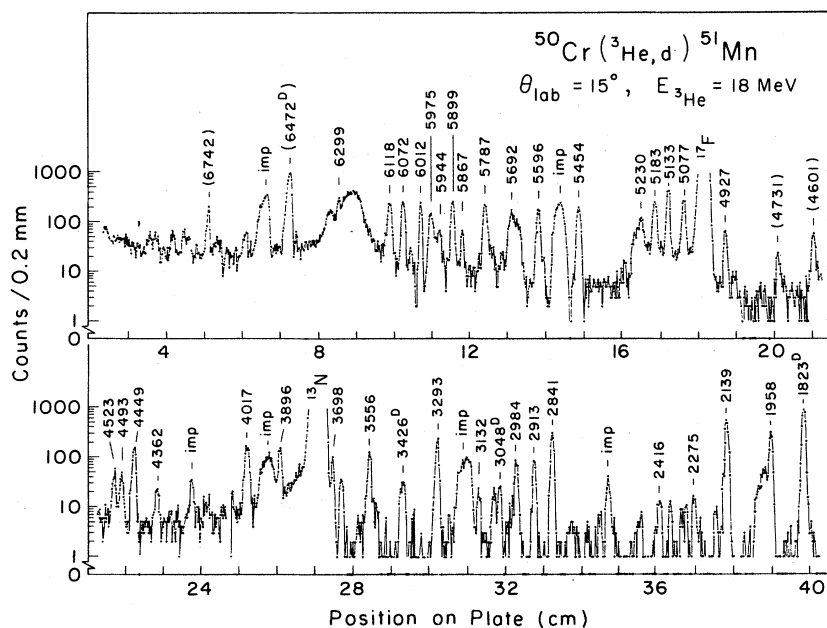


FIG. 2. Semilog spectrum of deuterons from $^{50}\text{Cr}(^3\text{He},d)^{51}\text{Mn}$ at $\theta_{\text{lab}} = 15^\circ$, taken with photographic emulsions. The bottom half of the spectrum contains most of the levels in ^{51}Mn spectroscopically analyzed in the present study. (The g.s. and the first excited state are not shown here.) The upper slice shows many strong unbound states, the energies of which are measured and listed in Table II. Some of the level energies shown in brackets refer to close doublets.

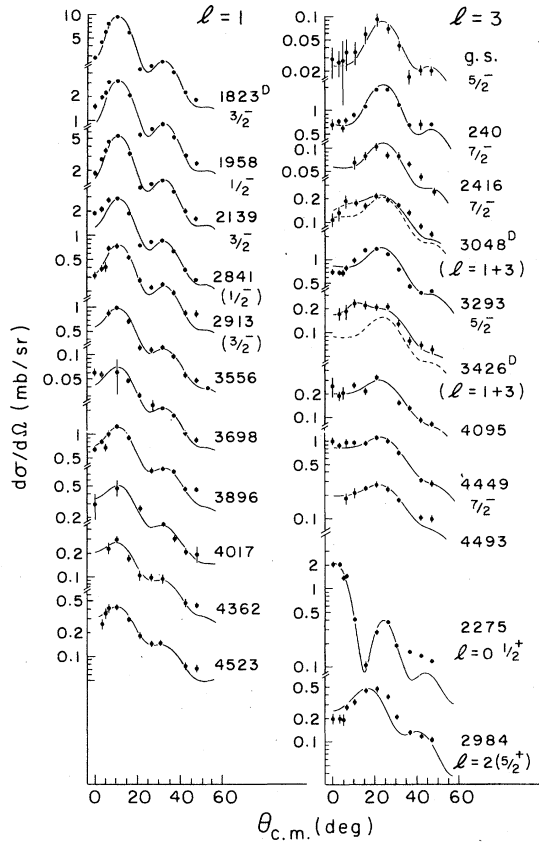


FIG. 3. Angular distributions for $^{50}\text{Cr}(^3\text{He}, d)^{51}\text{Mn}$ at $E_{^3\text{He}} = 18$ MeV compared with zero-range DWBA calculations. Unresolved, closely spaced doublets are indicated by the superscript *D*. DWBA curves are shown for the dominant *l* contributions. Error bars on the data points include all known and estimated random errors. The J^π values shown are assignments from other work (Refs. 20–22). Note that all known $\frac{3}{2}^-$ transitions agree well with the DWBA curves at all angles measured, whereas $l=1, j=\frac{1}{2}^-$ cross sections near zero degree are approximately 40% larger than DWBA predictions.

traction, and the random monitoring error which was $\leq 5\%$. Absolute cross-section scale errors are estimated to be $\pm 15\%$, mostly due to uncertainties in the target thickness and the spectrograph solid angle (1.2 msr).

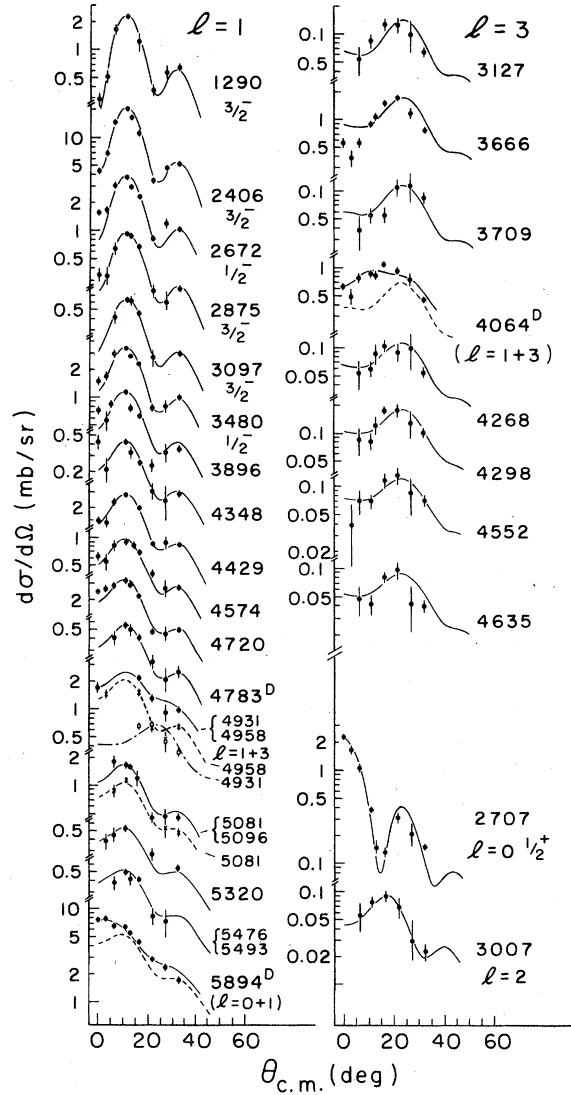


FIG. 4. Experimental angular distributions for the levels observed in the $^{52}\text{Cr}(^3\text{He}, d)^{53}\text{Mn}$ reaction compared with DWBA calculations. J^π values shown are taken from Ref. 20. Error bars on the data points include all known and estimated random errors. Note the good agreement of DWBA curves and data for the states known to have $\frac{3}{2}^-$ assignments, and the deviations near $\theta=0^\circ$ for $\frac{1}{2}^-$ angular distributions.

TABLE I. Optical-model parameters used in $^{50,52}\text{Cr}(^3\text{He}, d)^{51,53}\text{Mn}$ calculations.

	V (MeV)	r_0 (fm)	a_0 (fm)	W_D (MeV)	$4W_D$ (MeV)	r_I (fm)	a_I (fm)	V_{so} (MeV)	r_{so} (fm)	a_{so} (fm)	
18 MeV ^3He	165.3	1.20	0.65	16.7	0	1.60	0.80	6.0	1.15	0.63	Ref. 15
	152.7 ^a	1.20	0.72	39.1 ^a	0	1.40	0.88	6.0	1.20	0.88	Ref. 17
17.6 MeV d	92.20	1.15	0.79	0.04	54.95	1.33	0.736	5.5	1.10	0.55	Ref. 16
Bound proton	b	1.20	0.75					$\lambda = 25$			

^a Values given are for ^{52}Cr .

^b Well depth adjusted by code to fit proton separation energy.

TABLE II. Spectroscopic results for ^{51}Mn and comparison with previous work. Spin values in brackets are tentative, or (in column 3) indicate the j value chosen for the calculation of C^2S .

E_x^a (MeV)	Present work			$^{54}\text{Fe}(\phi, \alpha\gamma)^d$ (Ref. 18)			$^{50}\text{Cr}(\phi, \gamma)^e$ (Refs. 21, 22)			$^{50}\text{Cr}(^3\text{He}, d), E=12\text{ MeV}$ (Ref. 8)		
	l	J^π	$\left(\frac{d\sigma}{d\Omega}\right)_{\text{max}}$ (mb/sr)	C^2S^c	$C^2S(2J+1)$	E_x (MeV)	J^π	E_x (MeV)	l	J^π	l	J^π
0	3	$(\frac{5}{2}^-)$	0.09	0.03	0.15	0 ^d	$\frac{5}{2}^-$	0			$\frac{5}{2}^-$	
0.240	3	$(\frac{7}{2}^-)$	2.18	0.28	2.25	0.2374	$\frac{7}{2}^-$	0.240	3		$\frac{7}{2}^-$	2.33
1.138 ^f						1.1395	$\frac{3}{2}^-$	1.160				
1.488 ^f						1.4881	$\frac{11}{2}^-$	1.500				
1.823 ^g	1	$(\frac{3}{2}^-)$	9.38	0.16	0.63	1.8170	$(\frac{3}{2}^-)$	1.830	1			0.63
1.958	1	$(\frac{1}{2}^-)$	3.16	0.12	0.24	1.8246	$\frac{3}{2}^-$	1.962	1			0.21
2.139	1	$(\frac{3}{2}^-)$	5.39	0.09	0.36	1.9589	$\frac{1}{2}^-$	2.147	1			0.35
2.275	0	$\frac{1}{2}^+$	2.18	0.03(2S)	0.06	2.1403	$\frac{5}{2}^-$	2.2559				
2.416	3	$(\frac{7}{2}^-)$	0.12	0.01	0.08	2.2559	$\frac{1}{2}^-$	2.2759	0		$\frac{1}{2}^+$	$\left\{ \begin{array}{l} 0.06(2S) \\ 0.03(3S) \end{array} \right.$
2.841	1	$(\frac{1}{2}^-)$	2.95	0.11	0.22	2.3102	$(\frac{5}{2}^-)$	2.844	1			0.20
2.913	1	$(\frac{3}{2}^-)$	0.76	0.01	0.05	2.4159	$\frac{7}{2}^-$	2.9136	1			0.06
2.984	2	$(\frac{5}{2}^-)$	0.48	0.01(2d)	0.05	2.7015	$(\frac{5}{2}^-)$	2.9567				$\left\{ \begin{array}{l} 0.15(1d) \\ 0.06(2d) \end{array} \right.$
3.048 ^g	$\left\{ \begin{array}{l} (1) \\ (3) \end{array} \right.$		0.06 0.21	0.004 0.16		2.8414	$(\frac{1}{2}^-)$	3.0486	(1)			0.04
3.132 ^f	3	$(\frac{5}{2}^-)$	1.44	0.21	1.28	2.8930	$(\frac{5}{2}^-, \frac{1}{2}^-)$	3.052	3			0.84
3.293	(1)		0.14		0.01	2.9136	$(\frac{3}{2}^-)$	3.0915 ^e				0.03
3.426 ^g	(3)		0.16		0.11	2.9845	$\frac{5}{2}^-$	3.135	3			0.06
3.556	1		0.99		0.07	3.0486	$\frac{3}{2}^-$	3.300	(1)			0.06
3.698	(1)		0.71		0.05	3.4233	$\frac{5}{2}^-$	3.427	(1)			0.06
3.896	1		1.20		0.09	3.5530		3.555	1			0.09
4.017	(1)		0.50		0.04	3.6940		3.698	(0)			0.02(3S)
						3.8936		3.900				
						4.017		4.017				

TABLE II. (Continued)

^aThe estimated uncertainty is ± 2 keV for the levels below 3 MeV, ± 3 keV between 3 and 4.52 MeV. For the levels above 4.52 MeV the excitation energies were measured with an estimated uncertainty of ± 5 keV. (The existence of a small, systematic error in the energy calibration for these levels cannot be ruled out.)

^bThe estimated error in the absolute measured cross section is $\pm 15\%$. For the $l=0$ state the cross section at 0° is given.

^cSpectroscopic strengths are computed assuming the J^π values shown which—if unknown—were deduced from the j effect of their angular distributions. The average $C^2S(2J+1)$ value is given where J^π is uncertain.

^d J^π assignments and level energies below 3 MeV from Refs. 18 and 21.

^eExcitation energies between 3 and 5.6 MeV taken from γ -decay work (Ref. 22).

^fWeak state, only the excitation energy is measured.

^gUnresolved or poorly resolved doublet.

III. ANALYSIS AND RESULTS

In spite of improved energy resolution some close doublets remain unresolved, particularly in ^{53}Mn . Thus any search for a j dependence of the angular distributions must be limited to a few strongly excited states in both isotopes.

Experimental angular distributions are shown in Figs. 3 and 4. The curves represent distorted-wave Born-approximation (DWBA) calculations made with code DWUCK IV.¹⁴ For ^3He optical-model parameters, triton potentials with spin-orbit terms by Hardekopf *et al.*¹⁵ and for the deuterons global fit parameters by Childs *et al.*¹⁶ were used. The optical-model and proton-well parameters used are given in Table I. Zero-range DWBA calculations with nonlocality corrections of $\beta_{3\text{He}} = 0.25$ and $\beta_d = 0.54$ give very similar results for different sets of optical-model parameters, but all differ systematically from some of the experimental data. ^3He optical-model parameters from Becchetti and Greenlees¹⁷ used with the deuteron and proton potentials given in Table I yield angular shapes very similar to those obtained with the optical-model parameters by Hardekopf *et al.* But at small angles, curves calculated for the parameters of Ref. 17 lie slightly higher for the $l=1$ transfers (by $\leq 7\%$ at $\theta = 5^\circ$) and get flatter for $l=3$ as the excitation energies go higher. $l=3$ differences range from 6% to 15% at $\theta = 5^\circ$. The ^3He elastic cross sections derived from the global Becchetti-Greenlees ^3He potentials are about 13% smaller than those from Hardekopf *et al.*

The spectroscopic strengths obtained by normalizing the DWBA predictions to the experimental angular distributions and the deduced l values are listed in Tables II and III. A comparison with previously adopted level properties and the data of other studies^{11,18-22} is also given in the Tables.

IV. DISCUSSION

A. Evidence for j effects in $\text{Cr}(^3\text{He}, d)$

A study of Figs. 3 and 4 shows that most experimental angular distributions agree with the DWBA curves rather well. In fact on the basis of earlier ($^3\text{He}, d$) work⁸⁻¹² no dramatic disagreements would be expected, and any j dependence would have to be relatively small or at the extreme forward angles which have not been investigated previously. In looking for possible j effects it is therefore necessary to focus on data with very good statistics, particularly at small angles. For $l=1$ this limits us to the levels below 3.5 MeV. Out of a total of ten such $l=1$ transitions

TABLE III. Spectroscopic results for ^{53}Mn and comparison with previous work. Spin values shown in column 3 indicate the j value chosen for the calculation of C^2S .

E_x^a (MeV)	Present work			Nuclear data sheets (Ref. 20)			$^{52}\text{Cr}(^3\text{He}, d)$, $E=11$ MeV (Ref. 11)			
	l	J^π	$\left(\frac{d\sigma}{d\Omega}\right)_{\text{max}}^b$ (mb/sr)	C^2S^c	E_x (MeV)	J^π	E_x (MeV)	l	J^π	$C^2S(2J+1)$
0^d	3	$(\frac{1}{2}^-)$	2.29	0.38	0	$\frac{1}{2}^-$	0	3	$\frac{1}{2}^-$	4.1
0.378 ^d	(3)	$(\frac{5}{2}^-)$	(0.04)	(0.015)	0.3779	$\frac{5}{2}^-$	0.385		$(\frac{5}{2}^-)$	
1.290	1	$(\frac{3}{2}^-)$	2.32	0.05	1.2898	$\frac{3}{2}^-$	1.296	1	$(\frac{3}{2}^-)$	0.24
					1.4414	$\frac{11}{2}^-$				
					1.6199	$\frac{9}{2}^-$				
					2.2736	$\frac{5}{2}^-$				
2.406	1	$(\frac{3}{2}^-)$	20.8	0.36	2.4073	$\frac{3}{2}^-$	2.370	1	$(\frac{3}{2}^-)$	0.04
					2.5637	$\frac{13}{2}^-$		1	$(\frac{3}{2}^-)$	1.7
					2.5733	$\frac{7}{2}^-$				
2.672	1	$(\frac{1}{2}^-)$	3.86	0.15	2.6718	$\frac{1}{2}^-$	2.678	1	$(\frac{1}{2}^-)$	0.31
					2.6857	$\frac{5}{2}^-$, $\frac{1}{2}^-$				
					2.6935	$\frac{15}{2}^-$				
					2.6973	$\frac{11}{2}^-$				
2.707	0	$\frac{1}{2}^+$	2.20	0.03(2S)	2.707	$\frac{1}{2}^+$	2.720	0	$\frac{1}{2}^+$	0.05
					2.761?					
					2.839?					
					2.872?					
2.875	1	$(\frac{3}{2}^-)$	0.94	0.02	2.8769	$\frac{3}{2}^-$	2.882	1		0.09
					2.9134	$\frac{3}{2}^-$				
					2.9462	$(\frac{9}{2}^-)$				
					2.967?					
					2.978?					
3.007	2		0.09	$\left\{ \begin{array}{l} 0.01(1d_{5/2}) \\ 0.002(2d_{5/2}) \end{array} \right.$	3.0068	$(\frac{5}{2}^-)$		(2)	$(\frac{3}{2}^+)$	0.05
								(3)		0.08
3.097	1	$(\frac{3}{2}^-)$	0.63	0.01	3.0973	$\frac{3}{2}^-$	3.061	{ 3		0.13
					3.1036?		3.104	{ 1		0.06
3.127	3		0.14	0.03 ^h	3.1268	$\frac{5}{2}^-$, $\frac{1}{2}^-$, $\frac{3}{2}^-$				

TABLE III. (Continued)

E_x^a (MeV)	l	J^π	Present work		C^2S^c	Nuclear data sheets		E_x (MeV)	l	J^π	$C^2S(2J+1)$	$C^2S(2J+1)$
			$^{52}\text{Cr}(^3\text{He},d)^{53}\text{Mn}, E=18\text{ MeV}$	$\left(\frac{d\sigma}{d\Omega}\right)_{\text{max}}^b$ (mb/sr)		(Ref. 20)	(Ref. 11)					
3.480	1	$(\frac{1}{2}^-)$	3.41	0.13	0.25	$\frac{3}{2}^-$		3.484	1	$\frac{1}{2}^-$	0.30	
3.666	3		1.71	0.29 ^h	1.76 ^h	$\frac{5}{2}^-, \frac{1}{2}^-$		3.669	3		1.30	
3.709	(3)		0.12		0.10			3.7087				
3.896	1		1.16		0.08	$\frac{3}{2}^-, \frac{1}{2}^-$		3.900	1		0.08	
4.064 ^g	(1)		0.55		0.04			4.0653			0.06	
	(3)		0.69		0.52			4.0830			0.43	
4.268	(3)		0.12		0.08			4.278	3		0.92?	
4.298	3		0.18		0.13			4.304	3		0.16	
4.348	(1)		0.43		0.03			4.358	(0)	$(\frac{1}{2}^-)$	0.04	
4.429	1		2.81		0.19			4.434	1		0.22	
4.552	(3)		0.12		0.08			4.569	1		0.10	
4.574	1		0.98		0.07			4.721	1		0.28	
4.635	(3)		0.09		0.06			4.788	(0)	$(\frac{1}{2}^-)$	0.03	
4.720	1	$(\frac{1}{2}^-)$	3.30	0.12	0.24			4.936	3		0.29	
4.783 ^g	(1)		0.56		0.04			4.957	1		0.18	
4.931	(3)		0.66		0.42							
4.958	(1)		2.04		0.14							

TABLE III. (Continued)

E_x^a (MeV)		Present work $^{52}\text{Cr}(^3\text{He}, d)^{53}\text{Mn}$, $E = 18$ MeV $\left(\frac{d\sigma}{d\Omega}\right)_{\text{max}}$ (mb/sr)		Nuclear data sheets (Ref. 20)		$^{52}\text{Cr}(^3\text{He}, d)$, $E = 11$ MeV (Ref. 11)			
l	J^π	$C^3\text{S}^c$	$C^3\text{S}(2J+1)$	E_x (MeV)	J^π	E_x (MeV)	l	J^π	$C^3\text{S}(2J+1)$
5.081	(1)		0.12	5.085			1		0.12
5.096	(1)		0.04	5.322			(0)	$\left(\frac{1}{2}^+\right)$	0.03
5.320	(1)		0.04	5.485			1		0.05
5.476	(1)		0.04						
5.493									
(5.582) ^f									
(5.801) ^f									
5.894 ^g	{(0)		0.07(SS)	5.586					
5.954	{(1)		0.39	5.705					
(6.005) ^f				5.800					
				5.886					
				6.005					
				6.972					

^aThe estimated uncertainty is ± 2 keV below $E_x = 3$ MeV and ± 3 keV above 3 MeV except for the very weak levels at 5.582, 5.801, and 6.005 MeV which have an uncertainty of about ± 6 keV.

^dNot measured at all angles. Spectroscopic strengths are deduced from the data points at 10° and 25° using known spins.

^{b, c, e, f}See the corresponding footnotes for Table II.

^gThe values shown depend on the assumption $j = \frac{5}{2}$. For $j = \frac{7}{2}$ one obtains smaller values.

for the two isotopes we find that six are in excellent agreement with DWBA at all angles studied, whereas four transitions (those at 1958 and 2841 keV for ^{51}Mn , and at 2672 and, possibly, 3480 keV for ^{53}Mn) have small angle ($0-5^\circ$) cross sections up to 40% larger than predicted by DWBA. The disagreements are well outside of experimental uncertainties. All ten transitions have j assignments from previous γ -ray work (Refs. 18, 20-22) as shown in the figures. We note that the known $\frac{5}{2}^-$ transitions have angular distributions that show excellent agreement with DWBA. We also note that the four $l=1$ transitions singled out for their enhanced cross sections at zero degrees comprise all the known $p_{1/2}$ transitions. Hence the $l=1$ small-angle behavior of $(^3\text{He},d)$ is fully correlated with J of the final state (which here is identical to the j_p transfer).

For $l=3$ and $l=2$ transitions fewer documented j assignments exist. If we again confine ourselves to transitions with small experimental errors, the following observations can be made: Most $l=3$ data, but particularly all known $f_{7/2}$ transitions to ^{51}Mn levels (at 240, 2416, and 4449 keV) agree well with DWBA predictions; but significant disagreement is found for the strong 3293 keV level in ^{51}Mn and the 3666 keV level in ^{53}Mn . Both angular distributions are somewhat more structured and their stripping peaks seem shifted forward by about $3-4^\circ$ compared to their DWBA calculations. This is reminiscent of the $f_{5/2}$ shifts seen in (p,d) (Ref. 4) and (d,t) (Refs. 5, 6) reactions. The 3293 keV level has recently²¹ been assigned $\frac{5}{2}^-$ in γ -decay work. A comparison of the distribution of spectroscopic strength for ^{51}Mn (Fig. 5) and ^{53}Mn (Fig. 6) would suggest a similar parentage for the 3293 (^{51}Mn) and 3666 (^{53}Mn) $l=3$ transitions, but admittedly a larger set of known $\frac{5}{2}^-$ transitions would be needed to draw more than tentative conclusions about an $l=3$ j dependence.

Only two $l=2$ states are excited in this study. Only the $l=2$ calculation for the fairly strong 2984 keV level in ^{51}Mn (assigned $\frac{5}{2}^+$ in Ref. 21) is in significant disagreement with the data, which appear shifted backward by ~ 4 degrees. (The DWBA angular shapes are insensitive to $n=1$ or $n=2$ and $j=\frac{3}{2}$ or $j=\frac{5}{2}$ assumptions).

B. Spectroscopy of ^{51}Mn

The spectroscopic strengths $C^2S(2J+1)$ for ^{51}Mn states are listed in Table II and also shown graphically in Fig. 5. Their values were computed assuming the spins shown in brackets in Table I. Such spins were either known or assumed based on all available evidence. Where J^π remains quite

uncertain the average $C^2S(2J+1)$ value for the corresponding l value is given. Up to 4.5 MeV excitation about 45% of the $l=1$ and 59% of the $l=3$ theoretical strengths for T_z states²⁴ are observed. Values for $C^2S(2J+1)$ from the present study and Ref. 8 agree very well with each other. Figure 5 displays the measured distribution of the spectroscopic strengths. It can be seen from the spectrum of Fig. 2 that the missing strengths for $l=1$ and 3 are spread beyond $E^*=4.52$ MeV, especially over the many strong unbound states.

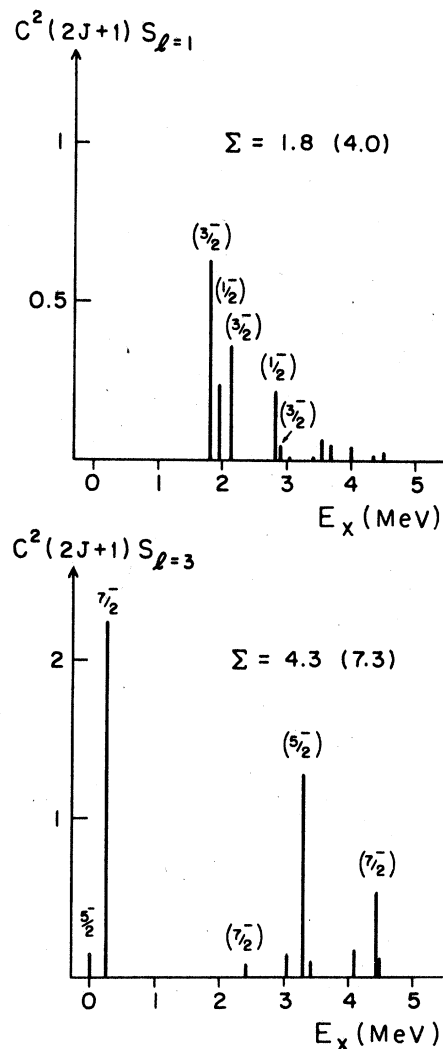


FIG. 5. Graphs of spectroscopic strengths for the $l=1$ and $l=3$ transfers in $^{50}\text{Cr}(^3\text{He},d)^{51}\text{Mn}$ up to 4.52 MeV. Averages of $p_{1/2}$ and $p_{3/2}$, or $f_{5/2}$ and $f_{7/2}$ DWBA calculations were used to extract strengths of peaks where J^π values are not identified. Note the wide distribution of the single-particle strengths and the missing strength for $l=1$ and 3 which is spread over still higher excited levels. Theoretical $\Sigma C^2S(2J+1)$ values for T_z states are given in brackets.

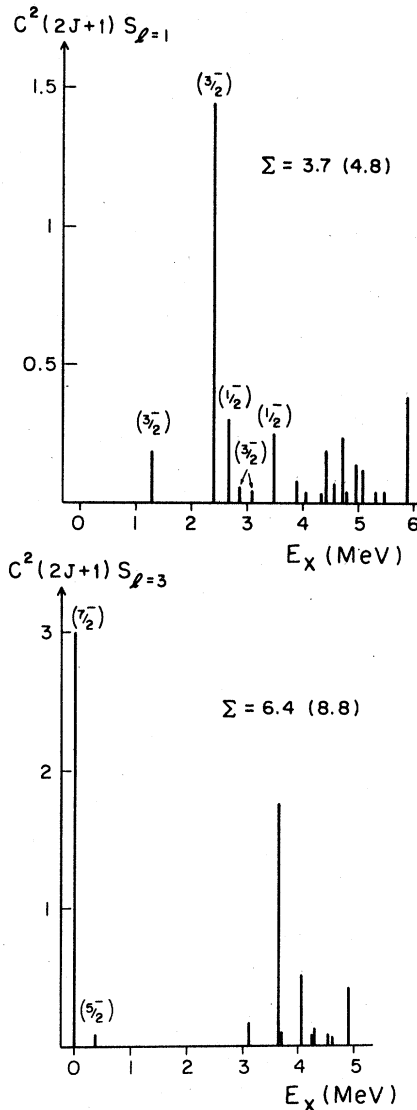


FIG. 6. Graphs of spectroscopic strengths for $^{52}\text{Cr}(^3\text{He},d)^{53}\text{Mn}$ up to 6 MeV. Also, see caption for Fig. 5.

The extraction of the spectroscopic strengths was limited to the levels below 4.52 MeV excitation energy, but we were able to get the excitation energies for 26 levels up to 6.74 MeV by use of spectra at five different angles.

A few conclusions in the literature were not confirmed by our data: Forsblom *et al.*²² and Noé *et al.*¹⁸ suggest that the 1.817 MeV level, the lower member of the doublet at 1.823 MeV, has positive parity with spin $\frac{5}{2}$ or $\frac{3}{2}$, respectively. This close doublet is observed in this $(^3\text{He}, d)$ study as a peak broader than singlet peaks at all angles; however, we could not find any indication for the existence of $l \neq 1$ transfer. Thus we be-

lieve that this doublet contains two $l=1$ states. Rapaport *et al.* report an $l=0$ state at 4.017 MeV, but our data show the level at this energy as an $l=1$ state (Fig. 3). Also they observed the levels at 3.058 and 3.427 MeV as the $l=1$ singlets, but in our study they are seen as doublets composed of $l=1$ and 3 after the subtraction of the contributions from the ^{53}Mn impurity states at 4.348 and 4.720 MeV, respectively. Another $l=1$ transfer is suggested for the weak level at 4.362 MeV.

C. Spectroscopy of ^{53}Mn

Our spectroscopic strengths deduced for ^{53}Mn levels tend to be slightly smaller than the corresponding values obtained by O'Brien *et al.*¹¹ (see Table III), but they are very comparable to the values compiled by Auble²⁰ from earlier $(^3\text{He}, d)$ data. Of the theoretically expected strengths $\Sigma C^2(2J+1)S$ for $T_<$ states (shown in parentheses in Fig. 6) 77% and 73% are seen for the $l=1$ and 3, respectively, up to $E^*=6$ MeV in ^{53}Mn . Fragmentation of single-particle strength over the higher excited states is similar to the ^{51}Mn case and the unobserved $l=1$ and 3 strength must lie in the levels beyond 6 MeV. Galès *et al.*²³ report an appreciable amount of the $l=1$ and 3 strengths for $T_<$ states between 7.0 and 8.5 MeV.

Comparison of the results of the present study with states adopted by NDS²⁰ for ^{53}Mn shows that below 4.1 MeV excitation many known ^{53}Mn states are not excited in the $^{52}\text{Cr}(^3\text{He}, d)$ reaction. Most of them are high spin ($l \geq 4$) states. The agreement with all other assignments is excellent. The ground state and the weak first excited state at 0.378 MeV were not measured at all angles. We deduced their spectroscopic factors from the data points at $\theta = 10^\circ$ and 25° using their known spins. We agree with Ref. 11 in most assignments, but differ in a number of cases: Three states above 4.3 MeV excitation assigned as $\frac{1}{2}^+$ in the $E_{\text{He}} = 11$ MeV study are observed as $l=1$ states in our analysis. An $l=0$ transfer was seen as a member of a close doublet at 5.894 MeV. The levels at 2.370 and 3.061 MeV reported in Ref. 11 were not seen. The spectroscopic strength (0.92) for the 4.278 MeV level¹¹ disagrees by an order of magnitude (possibly a typographical error). We resolved two $l=1$ doublets, with energies of 5.081 and 5.096 MeV and 5.476 and 5.493 MeV.

In view of the motivation of this study it is of particular interest to use our new $^{52}\text{Cr}(^3\text{He}, d)$ results for a reassessment of the earlier $^{52}\text{Cr}(^7\text{Li}, ^6\text{He})$ work of Ref. 2. The relatively low resolution of the ^7Li experiment (65–130 keV)² limits its usefulness to regions of low-level density. We deduce from our Fig. 1 and Table III

that conclusions for levels above 4 MeV excitation based on Ref. 2 (^7Li , ^6He) data would be difficult. However, for transitions to well-resolved final states the analysis with finite range DWBA calculations² appears to be successful. J assignments for the states at 0.000 MeV ($\frac{7}{2}^-$), 1.29 MeV ($\frac{3}{2}^-$), 2.41 MeV ($\frac{3}{2}^-$), 2.88 MeV ($\frac{3}{2}^-$), 3.48 MeV ($\frac{1}{2}^-$), and 3.67 MeV ($\frac{5}{2}^-$) are in perfect agreement with those found by other methods, including this ($^3\text{He},d$) study. Only the good $f_{5/2}$ fit to a peak at 3.06 MeV seems to be fortuitous. This peak should comprise the $l=2, 1$, and 3 triplet near 3.1 MeV which is unresolved in (^7Li , ^6He). We assume an $f_{5/2}$ assignment for the highest lying level (3.127 MeV) of this group; but the level at 3.097 MeV which is closest to the "3.06 MeV" value is known to be $\frac{3}{2}^-$ (Ref. 20). The relatively poor DWBA fit for the 2.68 MeV ($\frac{1}{2}^-$) level can be explained by an unresolved $\frac{1}{2}^+$ level at 2.70 MeV. Similarly, assignments made in Ref. 2 for the 4.07 and 4.43 MeV levels are weak, because the peaks in the ^6He spectra do not represent single levels. Nevertheless, we would conclude that where (^7Li , ^6He) angular distributions have been

obtained from peaks that now are known to contain single, resolved levels good DWBA fits and reliable J assignments were possible.

V. CONCLUSION

It is noted that our $^{50,52}\text{Cr}(^3\text{He},d)$ data at $E_{^3\text{He}} = 18$ MeV not only give the expected unique signature for the l_p transfer, but also seem to exhibit a small-angle j dependence. We find that a subset of our $l=1$ and $l=3$ angular distributions agrees very well with DWBA calculations (the $f_{7/2}$ and $p_{3/2}$ transitions) while the known $p_{1/2}$ and $f_{5/2}$ transfers differ in a systematic way. Spin assignments based on this j effect would agree with all previously assigned spin values. A number of new orbital angular momentum transfers for weakly excited states were assigned.

ACKNOWLEDGMENTS

This work has been supported by the National Science Foundation. We would like to thank Dr. R. M. DeVecchio and Dr. G. D. Gunn for their help in the data taking.

-
- ¹R. L. White, K. W. Kemper, L. A. Charlton, and G. D. Gunn, Phys. Rev. Lett. **32**, 892 (1974); K. W. Kemper, R. L. White, L. A. Charlton, G. D. Gunn, and G. E. Moore, Phys. Lett. **52B**, 179 (1974).
- ²G. D. Gunn, J. D. Fox, and G. J. KeKelis, Phys. Rev. C **13**, 595 (1976).
- ³L. L. Lee, Jr. and J. P. Schiffer, Phys. Rev. **136**, B405 (1964).
- ⁴R. Sherr, E. Rost, and M. E. Rickey, Phys. Rev. Lett. **12**, 420 (1964).
- ⁵R. H. Fulmer and W. W. Daehnick, Phys. Rev. Lett. **12**, 455 (1964); Phys. Rev. **139**, B579 (1965).
- ⁶W. W. Daehnick, Phys. Rev. **177**, 1763 (1969).
- ⁷J. E. Park, W. W. Daehnick, and M. J. Spisak, Bull. Am. Phys. Soc. **22**, 633 (1977).
- ⁸J. Rapaport, T. A. Belote, and W. E. Dorenbusch, Nucl. Phys. **A100**, 280 (1967).
- ⁹B. Cujec and I. Szöghy, Phys. Rev. **179**, 1060 (1969).
- ¹⁰D. D. Armstrong and A. G. Blair, Phys. Rev. **140**, B1226 (1965).
- ¹¹B. J. O'Brien, W. E. Dorenbusch, T. A. Belote, and J. Rapaport, Nucl. Phys. **A104**, 609 (1967).
- ¹²R. W. Tarata, J. D. Goss, P. L. Jolivet, G. F. Neal, and C. P. Browne, Phys. Rev. C **13**, 109 (1976).
- ¹³M. J. Spisak and W. W. Daehnick, Nucl. Instrum. Methods **153**, 365 (1978).
- ¹⁴DWBA code and instructions written by P. D. Kunz (unpublished) and extended by J. Comfort.
- ¹⁵R. A. Hardkopf, L. R. Veaser, and P. W. Keaton, Jr., Phys. Rev. Lett. **35**, 1623 (1975).
- ¹⁶J. Childs, W. W. Daehnick, and M. J. Spisak, Phys. Rev. C **10**, 217 (1974).
- ¹⁷F. D. Becchetti and G. W. Greenlees, *Proceedings of the Third (International) Symposium on Polarization Phenomena in Nuclear Reactions, Madison Wisconsin, 1970*, edited by H. H. Barschall and W. Haerberli (Univ. of Wisconsin, Madison, 1971), p. 682.
- ¹⁸J. W. Noé, R. W. Zurmühle, and D. P. Balamuth, Nucl. Phys. **A277**, 137 (1977).
- ¹⁹J. O. Jönsson, M. Olsmats, L. Sanner, and B. Wannberg, Nucl. Phys. **A166**, 306 (1971).
- ²⁰R. L. Auble, Nucl. Data Sheets, **21**, No. 3, 351 (1977).
- ²¹G. U. Din, J. A. Cameron, and R. G. Summers-Gill, Annual Report 1977, McMaster Accelerator Laboratory (unpublished).
- ²²I. Forsblom, T. Weckström, T. Sundius, G. Bergström, S. Forss, and G. Wansén, Phys. Scr. **6**, 309 (1972).
- ²³S. Galès, S. Fortier, H. Laurent, J. M. Maison, and J. P. Schapira, Phys. Rev. C **14**, 842 (1976).
- ²⁴J. B. French and M.H. Macfarlane, Nucl. Phys. **26**, 168 (1961).